High-resolution LiDAR and thermal UAV data for 3D analysis of urban vegetation structure and its cooling effect in San Nicolás, Mexico

Kevin David Rodríguez González [1], Aylet Vega-Aguilar [1,2], Fabiola Doracely Yépez-Rincón [1], Jacinto Treviño Carreón [3], Andrés Velastegui-Montoya [4], David Freire-Granda [4], Isabel Adriana Chuizaca Espinoza [4]

[1] Faculty of Civil Engineering, Department of Geomatics, Universidad Autónoma de Nuevo León, San Nicolás de los Garza, Nuevo León, México;

[2] Departament of Geography and Regional Planning, Institute for Research in Environmental Sciences of Aragon (IUCA), Universidad de Zaragoza, España

[3] Faculty of Engineering and Sciences, Universidad Autónoma de Tamaulipas, Ciudad Victoria, Tamaulipas, México

[4] Laboratory of Geoinformation and Remote Sensing, Faculty of Engineering in Earth Sciences, ESPOL Polytechnic University, Guayaquil, Ecuador

Keywords: LiDAR, UAV, thermal imaging, urban vegetation, 3D analysis, heat mitigation

Abstract

Urban vegetation is essential for mitigating the Urban Heat Island effect, yet its cooling performance depends on its three-dimensional structure. This study combines high-resolution Unmanned Aerial Vehicle - based LiDAR (Zenmuse L2) and thermal imaging (Zenmuse H20) to analyze vegetation structure and surface temperature across 4 urban parks in San Nicolás de los Garza, Mexico. LiDAR data were processed to generate Digital Terrain Model, Digital Surface Model and Canopy Height Model models, enabling the segmentation of individual trees and extraction of structural metrics such as canopy height, crown area and point density. Thermal orthomosaics were co-registered with LiDAR models to quantify temperature contrasts between vegetated and impervious areas. Results reveal consistent cooling effects in all parks, with vegetated zones showing 8–15 °C lower surface temperatures depending on canopy density and maturity. Larger parks with continuous canopies displayed the strongest thermal regulation. This integrated LiDAR–thermal approach provides a precise and scalable framework for assessing microclimatic benefits of urban vegetation, supporting climate-resilient planning in rapidly urbanizing regions.

1. Introduction

Urban Green Areas (UGAs) are essential components of urban ecosystems, functioning as critical infrastructure alongside transportation, education, and public services. These vegetated spaces, encompassing parks, gardens, street trees, and other forms of green infrastructure; play a vital role in promoting sustainable urban development (Ojobo et al., 2024). Their multifaceted benefits span environmental, social, and economic dimensions (Zhang & Qian, 2024; Oliveira et al., 2022), contributing to urban livability (Giannico et al., 2021) and enhancing ecosystem resilience (Vargas & Zdunek, 2021; Pamukcu, 2021).

However, rapid urbanization and the expansion of impervious surfaces have intensified the Urban Heat Island (UHI) effect, exacerbated temperature extremes and compromising thermal comfort in cities. Urban vegetation mitigates these effects by regulating microclimates through shading, evapotranspiration, and albedo modification (Bowler et al., 2010; Ziter et al., 2019). Despite its crucial role, the value of UGAs is often underestimated in urban decision-making (Giuliani, 2021), and their spatial distribution and ecological functionality remain poorly documented in many rapidly growing cities (Odhengo et al., 2024).

Reliable, high-resolution data on the spatial extent, structural complexity, and temporal dynamics of UGAs are therefore essential for effective urban planning and management. Accurate inventories enable evidence-based decisions concerning maintenance priorities, green infrastructure expansion, and the evaluation of ecological services such as microclimate regulation, biodiversity support, and carbon sequestration (Verdú, 2021; Wang, 2023; Godoi et al., 2025). Without such data, municipalities struggle to monitor environmental change and plan equitable access to green infrastructure.

Traditional forest inventories, based on plot-level sampling, provide valuable ecological indicators such as species composition, height, canopy spread, and biomass (Zheng et al., 2021). However, their limited spatial coverage restricts their usefulness for urban-scale assessments. Recent advances in Terrestrial Laser Scanning (TLS) have improved forest characterization at centimeter-level precision (Xi et al., 2022), yet their applicability remains constrained by high operational costs and limited spatial reach.

In contrast, Unmanned Aerial Vehicles (UAVs) have emerged as flexible and cost-effective remote sensing platforms for mapping urban vegetation. Equipped with advanced sensors including LiDAR and thermal cameras UAVs enable high-resolution three-dimensional (3D) characterization of vegetation structure and its microclimatic effects (Yang et al., 2022; Yan et al., 2021). The integration of multi-sensor UAV data supports detailed analysis of canopy morphology, vegetation density (Rodríguez et al., 2025), and surface temperature, providing new opportunities for understanding how vegetation structure influences urban thermal dynamics.

Although UAV-based remote sensing studies have rapidly expanded in Asia, North America, and Europe, Latin American cities remain underrepresented in high-resolution analyses of

https://doi.org/10.5194/isprs-archives-XLIX-B3-2026-421-2026

urban vegetation structure and its thermal performance. Most existing studies focus either on 3D vegetation characterization or on land surface temperature mapping independently, limiting the understanding of how canopy geometry influences microclimatic regulation. The integration of LiDAR-derived structural metrics with thermal orthomosaics provides an opportunity to better quantify the role of vegetation morphology in mitigating urban heat, particularly in rapidly urbanizing and climatically vulnerable regions.

The use of UAV-based data also aligns directly with the United Nations Sustainable Development Goal (SDG) 11**,** particularly Target 11.7, which aims to ensure universal access to safe, inclusive, and accessible green and public spaces by 2030. High-resolution 3D and thermal datasets can therefore inform equitable green space planning and assess the contribution of vegetation to urban resilience and climate adaptation.

Building on this context, this study focuses on the integration of LiDAR and thermal UAV data to analyze the relationship between vegetation structure and surface temperature across 4 urban parks in San Nicolás de los Garza, Mexico.

Although previous studies have independently applied UAV-based LiDAR or thermal imaging to analyze vegetation structure or surface temperature, integrated approaches that combine high-resolution 3D structural metrics with radiometrically calibrated thermal data remain limited, especially in Latin American cities characterized by rapid urbanization and semi-arid climatic conditions.

This study contributes to the existing literature by proposing an operational and scalable workflow that integrates UAV-based LiDAR and thermal imaging to quantify the relationship between vegetation structure and microclimatic regulation in multiple urban green spaces. Unlike studies focused solely on geometric characterization or temperature mapping, this research combines segmentation, canopy structural metrics, and spatially explicit thermal information to assess the cooling performance of urban vegetation at the municipal scale.

The main contributions of this study are:

- Integration of structural variables derived from high-resolution LiDAR (canopy height, crown area, and point density) with radiometrically calibrated thermal orthomosaics.
- Application of a consistent multisensor workflow using UAVs in 4 urban green spaces representing heterogeneous urban conditions.
- Quantitative assessment of the relationship between vegetation structure and surface temperature reduction in a semi-arid urban environment.
- Development of a replicable methodological framework that can support climate-resilient urban planning and evidence-based green infrastructure management.

2. Methodology

2.1 Study area

The study was conducted in San Nicolás de los Garza, a municipality located in the central-western region of the state of Nuevo León, Mexico (Figure 1). It borders the municipalities of Apodaca and General Escobedo to the north and Monterrey and Guadalupe to the south. With an area of approximately 86.8 km², San Nicolás represents less than 1 % of the state's total surface, making it the third smallest municipality in Nuevo León. Despite its limited geographic extent, it supports a dense urban population of about 412,800 inhabitants.

Geographically, San Nicolás lies at the foothills of the Sierra Madre Oriental, at an average elevation of 500 m a.s.l**.** The local climate is semi-arid and warm, with mean maximum temperatures reaching around 40 °C in May and an annual average of 550 mm of precipitation. Rapid urban expansion and limited vegetated surfaces have led to significant heat-island effects within the municipality, highlighting the importance of studying the thermal contribution of its remaining urban parks.

For this research, 4 UGAs were selected across the municipality (Figure 1). These parks vary in size, vegetation density, and spatial configuration, representing a range of urban micro-environments. Their selection was based on accessibility, distribution, and the presence of significant tree coverage, ensuring a representative sample of San Nicolás's green infrastructure network.

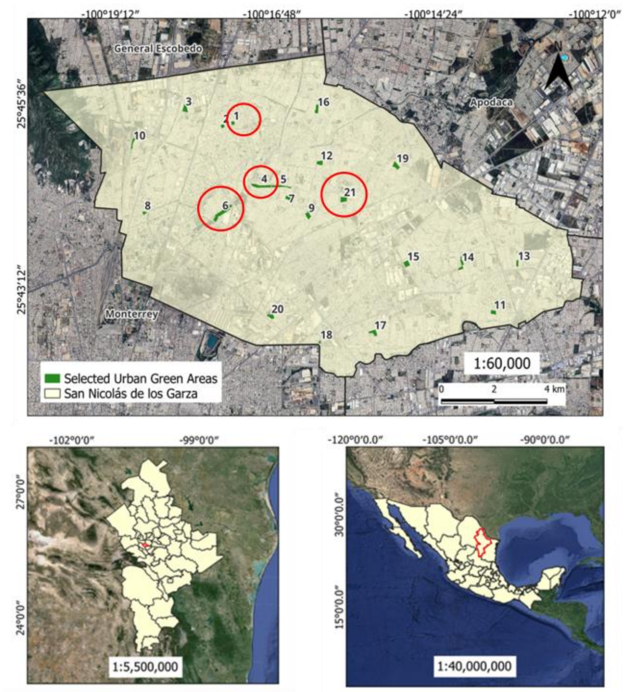

Figure 1. Location of urban green areas (UGA) in the municipality of San Nicolás de los Garza, Nuevo León, México. Selection of 4 representative areas for the study.

High-resolution UAV-based data were later used to analyze vegetation structure and surface temperature within these parks, providing a consistent spatial basis for subsequent three-dimensional and thermal analysis.

2.2 Overview

The proposed methodology aims to provide a reproducible workflow for integrating LiDAR and thermal datasets acquired with UAVs to evaluate the structural factors influencing urban cooling effects. The workflow prioritizes consistency across multiple urban green spaces to enable comparative analysis of vegetation morphology and its influence on spatial temperature variability.

Both campaigns were conducted between July and August 2024 using a DJI Matrice 350 RTK platform, which ensured high spatial accuracy through RTK-GNSS correction and consistent flight planning over the 4 urban parks of San Nicolás de los Garza, Mexico

The overall workflow for UAV data acquisition and processing is summarized in Figure 2. The process included pre-flight planning, on-site inspection, and post-flight data processing to generate three-dimensional UGA models. This sequence ensured consistent data quality and facilitated subsequent vegetation segmentation and structural analysis.

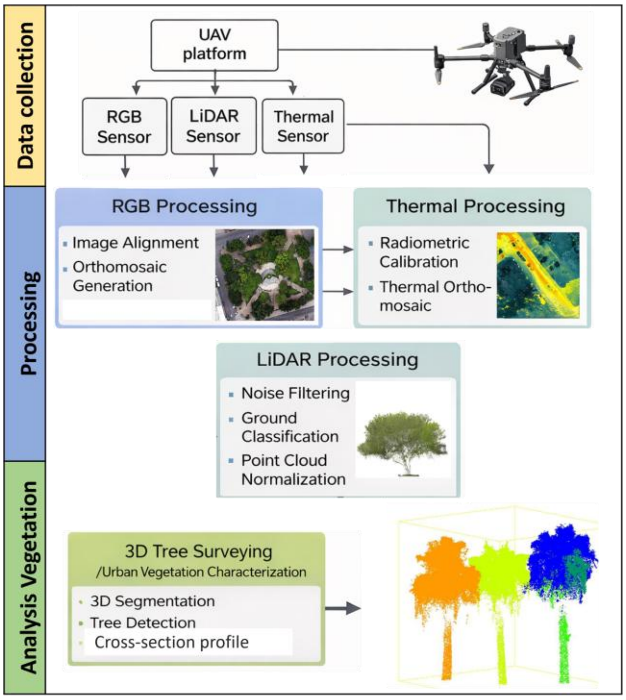

Figure 2. General workflow for UAV-based data acquisition, processing, and 3D modeling of urban green areas (UGAs).

2.3 LiDAR Data acquisition

LiDAR data were acquired using a Zenmuse L2 sensor mounted on the Matrice 350 RTK (Figure 2). The Zenmuse L2 is a high-precision aerial laser scanner equipped with a 905 nm laser, capable of recording up to five returns per pulse and achieving a ranging accuracy of 2 cm (RMS 1σ) within 150 m. The unit integrates a 4/3 CMOS RGB camera (20 MP) that supports visual context and colorization of the point cloud.

Flights were executed at altitudes of 90-100 m AGL with 75-80 % overlap between flight paths. Each mission covered approximately 3 ha per park. Weather conditions were clear, with average air temperatures around 20 °C and wind speeds below 6 km h^{-1}, minimizing positional drift and vegetation motion artifacts.

The LiDAR system recorded dense point clouds at a rate of up to 240,000 points s^{-1}, capturing detailed vertical vegetation structure, including canopy, understory, and ground returns. All data was stored in LAS 1.4 format for post-processing.

2.4 LiDAR Data processing

LiDAR data processing was performed in CloudCompare, following four main steps (CloudCompare, 2025):

- Noise filtering and classification: Raw point clouds were filtered to remove outliers and erroneous returns.
- Ground classification: Ground points were extracted using the Cloth Simulation Filter (CSF) (Zhang et al., 2016) to produce a high-accuracy Digital Terrain Model (DTM).
- Surface modeling: A Digital Surface Model (DSM) was generated from first returns to capture canopy and built-surface elevations (Vega et al., 2025).
- Canopy Height Model (CHM): Vegetation height was normalized according to providing a continuous surface of canopy heights. The CHM was calculated using equation (1) where:

$$CHM = DSM - DTM, \tag{1}$$

where CHM = Canopy Height Model
DSM = Digital Surface Model
DTM = Digital Terrain Model

Tree-Crown Segmentation and Structural Metrics

Individual tree crowns were delineated in CloudCompare using a hierarchical segmentation workflow based on the TreeISO algorithm (Xi & Hopkinson, 2022).

- Initial segmentation: local clusters identified through a *k*-nearest neighbor search (*k = 5*).
- Intermediate merging: clusters combined horizontally via a 2D cut-pursuit algorithm (Landrieu & Obozinski, 2017) with a 2 m spatial gap threshold.
- Final refinement: vertical overlap and canopy geometry evaluated to separate adjoining crowns.

The k-nearest neighbor parameter (k = 5) was selected based on previous applications of TreeISO segmentation in complex vegetation structures (Xi & Hopkinson, 2022), where low k-values have been shown to improve crown separation in heterogeneous urban environments. The spatial gap threshold of 2 m was defined considering typical crown spacing observed in urban parks, allowing separation of adjacent trees while avoiding over-segmentation of continuous canopy clusters.

The rasterization of LiDAR-derived metrics to 1 m spatial resolution was chosen to balance spatial detail and computational efficiency, while maintaining compatibility with the spatial resolution of thermal orthomosaics. This resolution has been widely used in urban vegetation studies to ensure consistent integration between structural and thermal datasets.

From each segmented crown, the following structural attributes were extracted:

- Maximum height (Hmax),
- Canopy area (Acan), and
- Point density (Dpts).

2.5 Thermal Data acquisition

Thermal imaging was performed using the Zenmuse H20 sensor mounted on the same UAV platform during a separate flight campaign. The H20 integrates a 20 MP CMOS RGB camera and a radiometric thermal module capable of detecting surface temperatures within a range of -20 °C to 50 °C.

Flights were conducted at 60-80 m AGL during 09:00-11:00 a.m. under clear sky conditions to minimize thermal distortion. Each park was surveyed in a single mission, maintaining the same flight overlap and coverage pattern as the LiDAR survey to facilitate later co-registration. Ambient air temperature and relative humidity were recorded during each mission for radiometric correction.

2.6 Thermal Data processing

Thermal imagery was processed in ArcGIS Pro, including:

- Radiometric calibration to convert digital numbers to absolute temperature (°C)
- Orthomosaic generation and georeferencing
- Co-registration with LiDAR-based CHM using RTK-derived ground-control points (accuracy < ± 2 cm)

For each park, thermal statistics were extracted from vegetated and non-vegetated areas. Mean (Tmean) and maximum (Tmax) surface temperatures were calculated per tree crown and its adjacent impervious zone. These values were later compared against LiDAR-derived canopy metrics to quantify vegetation-induced cooling effects.

Co-registration between thermal orthomosaics and LiDAR-derived CHM was performed using RTK-GNSS ground control points with horizontal accuracy better than ±10 cm. Thermal data were resampled to 0.05 m spatial resolution using bilinear interpolation to ensure spatial correspondence with LiDAR-derived raster products. This spatial resolution was selected to preserve relevant temperature variability while minimizing noise associated with very high-resolution thermal pixels.

2.7 Field validation

A complementary botanical field survey was conducted during the UAV campaigns to validate vegetation classification (Figure 3). Dominant species were identified *in situ* and georeferenced. These data were used to confirm the positional and thematic accuracy of LiDAR-derived crowns and to characterize local vegetation types.

Figure 3. Field validation of vegetation classification in UGA-1, showing representative tree species identified in situ during the UAV survey.

2.8 Data Integration and analysis

The LiDAR and thermal datasets obtained during the flights (Table 1) were integrated into ArcGIS Pro. Mesh statistics were obtained in ArcGISSoft metashape (Table 2). Spatial overlays allowed direct comparison of structural and thermal variables. Correlation and regression analyses were performed to explore relationships between canopy height, crown area, and temperature reduction.

This integrated analysis provided quantitative evidence of how vegetation geometry influences microclimatic regulation across the 4 urban parks.

Parameter	LiDAR (Zenmuse L2)	Thermal (Zenmuse H20)
Flight altitude	90–100 m AGL	60–80 m AGL
Image/point overlap	75–80 %	75–80 %
Average surveyed area per mission	≈ 3ha	≈ 3ha
Sensor precision	2 cm (RMS 1σ)	± 2 °C radiometric accuracy
Max returns per pulse	5	–
Point rate / Resolution	≤ 240 000 ptos s^{-1}	3840 × 2160 px
Spectral range / band	905 nm laser	8–14 µm thermal band
Average processing time per park	≈ 35 min	≈ 25 min

Table 1. Summary of UAV flight and processing parameters

https://doi.org/10.5194/isprs-archives-XLIX-B3-2026-421-2026

3. Results

3.1 Processing and calculation

The results presented in this study are specifically focused on four distinct UGAs within the municipality of San Nicolás (1, 4, 6 and 21). These selected UGAs were chosen to represent the heterogeneity observed across the city's green spaces, encompassing variations in size, vegetation structure, management practices, and surrounding urban context (Figure 4 and 5). By focusing on these examples, this study aims to provide insights into the range of characteristics and ecological conditions present within the broader spectrum of UGAs in San Nicolás.

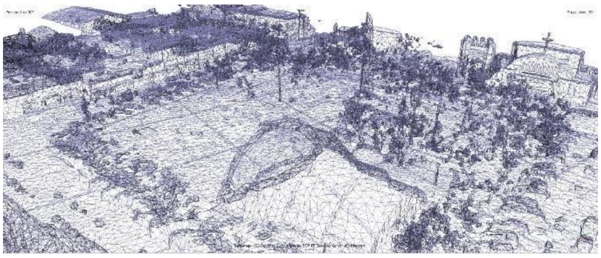

Figure 4. Three-dimensional mesh model generated from LiDAR point cloud data for UGA-1. The mesh representation illustrates the geometric structure of terrain and vegetation, providing a detailed visualization of canopy morphology prior to segmentation.

Vegetation ground separation was performed in CloudCompare using a geometry-based filtering workflow optimized for natural surfaces. First, the raw point cloud was processed with the CSF, which simulates an inverted flexible surface draped over the terrain to distinguish ground returns from elevated objects.

Property	Value
Total faces	9371203
Total	4713461
Similar vertices	2634
Degenerated faces	14
Open edges	477
Connected components	18766

Table 2. Mesh statistics UGA-1

The algorithm was executed under the “Outdoor” configuration with a cloth resolution of 0.3–0.5 m and a classification threshold, enabling the reliable identification of structural discontinuities associated with vegetation. This procedure yielded two subsets ground and non-ground points from which the non-ground class was further refined through relative height calculations to remove low-lying noise and isolate vegetative elements.

Figure 5. (a) Raw 3D LiDAR point cloud of UGA-1 and (b) non-ground points extracted using the Cloth Simulation Filter (CSF) algorithm. The filtering process separates terrain points from vegetation returns

3.2 Tree crown segmentation

3.1.1 UGA-1 analysis: The Bernardo Reyesico main square in San Nicolás (Figure 6) features established vegetation of mature trees bordering a paved central area.

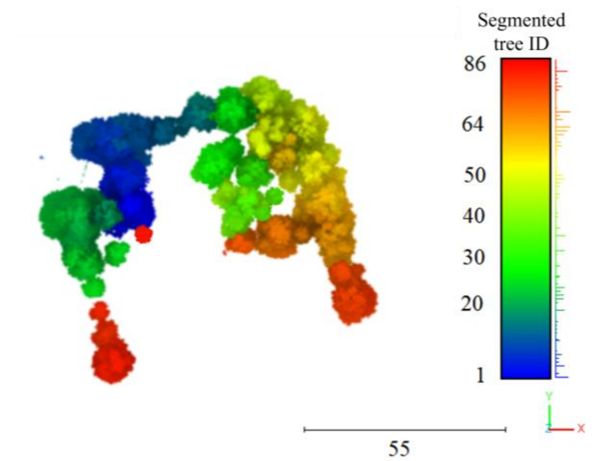

Figure 6. Individual tree crown segmentation in UGA-1 derived from LiDAR point cloud data using the TreeISO algorithm. Each color corresponds to a unique tree identifier (Tree ID), allowing visual differentiation of individual canopies.

The segmentation of the point cloud data of UGA-1 resulted in the identification of a total of 86 individual trees (Figure 6). These segmented trees were represented by 3,777,445 individual 3D points. The distribution of point density across the trees revealed considerable variability, with a high presence of trees with more extensive canopies, greater height or more complex structure (Figure 7).

https://doi.org/10.5194/isprs-archives-XLIX-B3-2026-421-2026

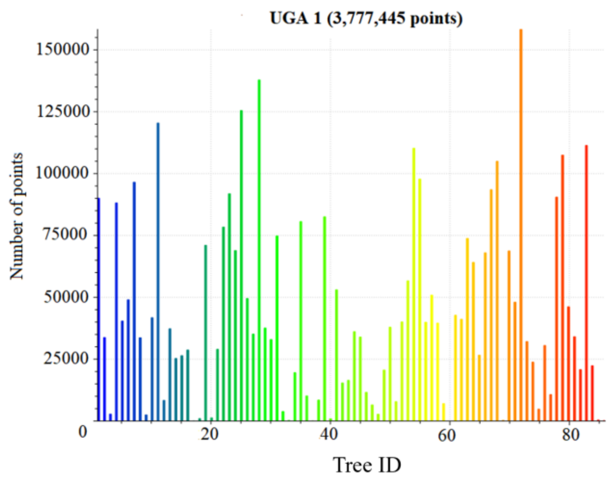

Figure 7. Distribution of LiDAR point density for individual segmented trees in UGA-1. Each bar represents a unique tree identifier (Tree ID), illustrating variability in canopy structural complexity captured by the LiDAR survey.

3.1.2 UGA-4 analysis: Las Arboledas functions primarily as an elongated park and is characterized by a continuous, mature tree canopy that includes centuries-old trees.

The tree isolation process to the point cloud of UGA-4 yielded a count of 90 individual trees (Figure 8). These segmented trees were characterized by a dataset comprising 4,051,520 3D points. An examination of the point distribution across the individual trees indicated the presence of trees exhibiting a high point density, over 100,000 points, suggesting well-defined structural attributes and potentially larger or more intricate canopies.

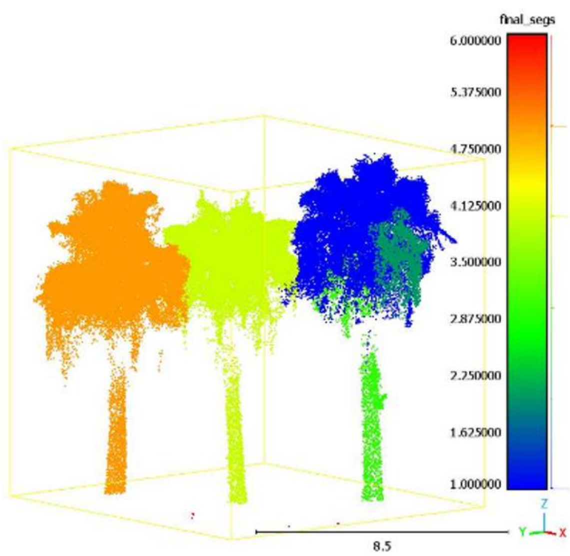

Figure 8. Point density distribution among trees in UGA-4

3.1.3 UGA 6 analysis: The Gran Parque San Nicolás, characterized by extensive green areas, various sports facilities, and groups of mature trees strategically distributed throughout the park.

The segmentation of the extensive point cloud of Gran Parque San Nicolás revealed a substantial count of 948 individual trees. These trees were represented by a massive collection of 59,048,412 3D points, underscoring the scale and complexity of the park's vegetation. Notably, the analysis of the point density distribution across these segmented trees indicates a significant presence of densely represented vegetation, with a considerable number of individual trees exhibiting point counts exceeding one million. This suggests the presence of numerous large, structurally complex, and well-defined trees within Gran Parque San Nicolás, contributing to its rich and varied vegetative character.

3.1.4 UGA 21 analysis: It offers a localized green space and functions as a green corridor, contributing to the local microclimate.

The tree segmentation process to UGA 21 resulted in the identification of 75 individual trees. These trees were represented by a total of 352,425 3D points. The relatively low total point count, coupled with the number of identified trees, suggests that the average point density per tree is considerably lower compared to larger UGAs. This indicates that the trees within UGA 21 are likely smaller in stature, possess less complex canopy structures, or a combination of both, resulting in fewer laser returns captured during the point cloud acquisition.

3.3 Tree crown structural analysis results

The comparative analysis of four UGAs within San Nicolás revealed distinct characteristics in their tree populations based on mean point density, mean area, and mean height (Table 3). UGA 4 exhibits the highest mean point density (74,418.6 points), suggesting trees with more complex structures and/or denser foliage, coupled with the largest mean area (183.9 m²) and the greatest mean height (7.7 m). This indicates that the trees in UGA 4 are, on average, larger and more structurally detailed in the point cloud compared to the other UGAs. In contrast, UGA 21 displays a significantly lower mean point density (4,894.8 points), along with the smallest mean area (32.2 m²) and mean height (3.1 m), suggesting a prevalence of smaller trees with less intricate structures in this UGA.

UGA	Mean point density	Mean area (m²)	Mean height (m)
1	49,058	41.7	5.1
4	74,418.6	183.9	7.7
6	67,716.1	44.5	4.9
21	4.894.8	32.2	3.1

Table 3. UGAs structural analysis

UGAs 1 and 6 present intermediate characteristics. UGA 1 shows a mean point density of 49,058 points, a mean area of 41.7 m², and a mean height of 5.1 m, indicating trees of moderate size and structural complexity. Similarly, UGA 6 has a mean point density of 67,716.1 points, a mean area of 44.5 m², and a mean height of 4.9 m, suggesting trees with relatively high point density but moderate size. These findings highlight the heterogeneity in tree characteristics across different UGAs within the same municipality, likely influenced by factors such as park age, management practices, species composition, and surrounding urban context.

3.4 Intensity

The intensity distribution of LiDAR returns allowed for the identification of significant variations in foliage density and structure within UGA-1. In general, canopies with high intensity values correspond to areas with a greater number of leaves and less light penetration, indicating denser and more continuous canopy cover. Conversely, lower intensity values are associated with open canopies, structural gaps, or areas with less leaf cover. This relationship between intensity and foliage density is relevant from a microclimatic perspective: dense canopies generate more shading and reduce direct radiation on the ground, resulting in lower surface temperatures. Thus, LiDAR intensity not only describes the internal structure of the canopy but also helps explain the thermal patterns observed in vegetated areas, where shade and leaf mass act as urban heat sinks (Figure 9).

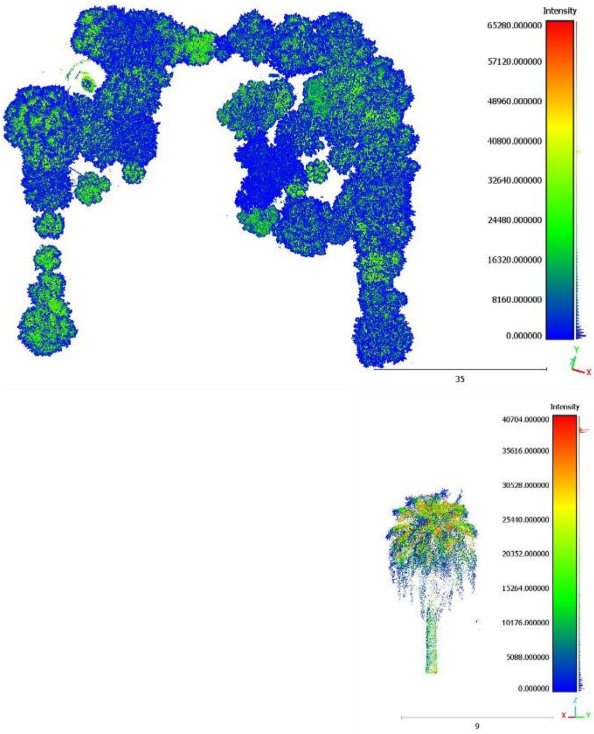

Figure 9. Spatial distribution of LiDAR intensity and point density among trees in UGA-1, shown in plan view and cross-sectional profile.

3.5. Thermal

The radiometric analysis of the captured thermal imagery, as exemplified in Figure 10, revealed significant surface temperature heterogeneity within the urban environment. The calibrated thermogram shows a temperature range spanning from 22°C to 42°C. A clear thermal dichotomy was observed between impervious and pervious surfaces. Impervious materials, including the asphalt pavement and vehicles, exhibited the highest surface temperatures, corresponding to the yellow, orange, and red signatures.

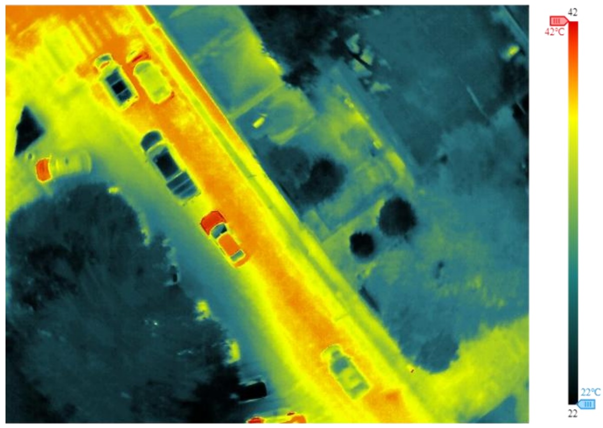

Thermal Image Parameters

Humidity	50%
Emissivity	0.95
Reflected Temp	25.0°C

Figure 10. Radiometrically calibrated thermal orthomosaic of UGA-1, acquired with the Zenmuse H2O sensor, illustrates the spatial variability of Earth's surface temperature.

Conversely, the vegetation canopy and associated shadowed areas consistently registered the lowest temperatures within the scene, appearing as dark blue to black, which aligns with the 22°C lower bound of the thermal scale (Figure 10).

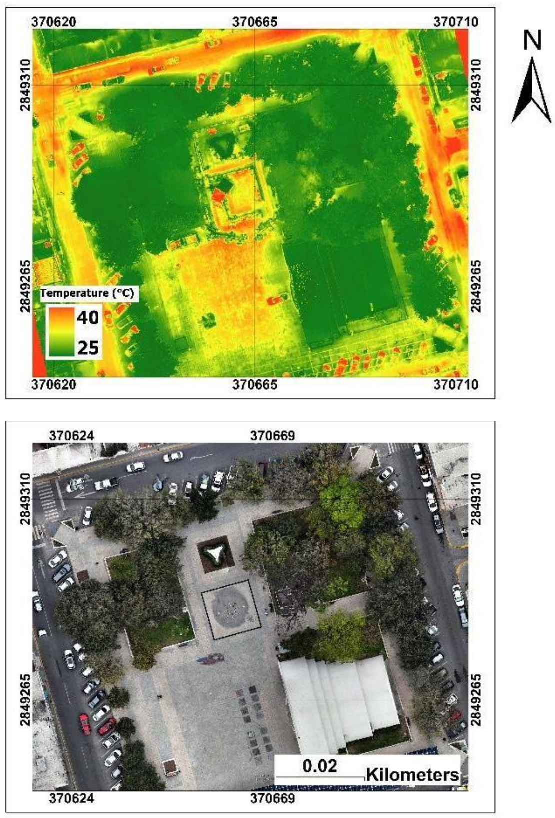

Figure 11. RGB and thermal orthomosaics of UGA-1. Cooling effect of the tree canopy in relation to the surrounding impermeable urban surfaces.

The radiometric thermal data acquired with the DJI sensor reveal a pronounced spatial heterogeneity in surface temperatures across the surveyed urban park (Figure 11). High-temperature zones exhibit elevated radiative absorption, low emissivity, and significant thermal inertia, resulting in rapid heat accumulation under direct solar exposure.

In contrast, vegetated areas including tree canopies and dense grass consistently display the lowest temperatures due to evapotranspirative cooling and shading effects, underscoring their fundamental role as microclimatic regulators. This thermal differentiation produces a distinct boundary between the vegetated core and surrounding built infrastructure, where surface temperatures increase abruptly when transitioning from green cover to hardened urban materials

4. Conclusions

The application of UAV-based surveying and subsequent analysis, as demonstrated across the four UGAs in San Nicolás, highlights the significant potential of this technology for efficient and detailed urban green space inventories. The ability to rapidly acquire high-resolution 3D data allows for the accurate identification and segmentation of individual trees, even in complex urban environments. Furthermore, the derived metrics, such as point density, crown area, and tree height, provide quantitative insights into the structural characteristics of urban vegetation at an individual tree level, surpassing the limitations of traditional ground-based surveys or coarser resolution satellite imagery. This detailed information is crucial for effective monitoring, management, and planning of urban green infrastructure.

The variability observed across the analyzed UGAs underscores the utility of UAV-based inventories in capturing the heterogeneity inherent in urban forests. From the dense, mature vegetation of Las Arboledas and Gran Parque San Nicolás to the smaller, less complex trees of UGA 21, the detailed point clouds and derived metrics effectively differentiate these distinct characteristics. This level of resolution enables a more appropriate understanding of the ecological contributions and management needs of individual UGAs within a city. Consequently, UAV-based inventories offer a powerful tool for urban planners and environmental managers at the municipal level to make informed decisions regarding the conservation, expansion, and sustainable management of their vital urban green spaces.

Furthermore, thermal analysis confirmed that the effectiveness of parks in moderating urban heat depends directly on the three-dimensional structure of the trees. Areas with continuous canopies, mature trees, and high leaf density registered significant surface temperature reductions, between 8 and 15 °C compared to impermeable surfaces, while parks with fragmented or shorter vegetation showed limited thermal benefits. This behavior demonstrates that canopy shape, height, and continuity are key factors in urban microclimate regulation.

Beyond site-specific results, the proposed workflow demonstrates how the integration of UAV-based LiDAR and thermal data can provide transferable indicators of vegetation cooling performance, supporting standardized assessment of urban green infrastructure in data-scarce regions.

Acknowledgements

The authors thank the Secretariat of Science, Humanities, Technology and Innovation (SECIHTI) for the scholarships awarded to the Doctoral students who, through the Postgraduate Program of the Faculty of Civil Engineering of the Autonomous University of Nuevo León, have acquired the skills to partially support this type of project, as well as the Department of Geomatics of the Institute of Civil Engineering for providing the tools and resources necessary to carry out this research.

References

CloudCompare (version 2.14) [GPL software], 2025: Retrieved from http://www.cloudcompare.org/

Bowler, D. E., Buyung-Ali, L., Knight, T. M., Pullin, A. S. (2010). Urban greening to cool towns and cities: A systematic review of the empirical evidence. *Landscape and Urban Planning, 97, 3*. https://doi.org/10.1016/j.landurbplan.2010.05.006

Giannico, V., Spano, G., Elia, M., D’Este, M., Sanesi, G., & Lafortezza, R, 2021: Green spaces, quality of life, and citizen perception in European cities. *Environmental Research*, 196, 110922.

Giuliani, G., Petri, E., Interwies, E., Vysna, V., Guigoz, Y., Ray, N., & Dickie, I, 2021: Modelling accessibility to urban green areas using Open Earth Observations Data: A novel approach to support the urban SDG in four European cities. *Remote Sensing*, 13(3), 422.

Godoi, N. M. I., Gomes, R. C., & Longo, R. M., 2025: Contributions of urban green spaces to cities: A literature review. *Sustainable Environment*, 11(1), 2464418.

Landrieu, L., & Obozinski, G., 2017: Cut pursuit: Fast algorithms to learn piecewise constant functions on general weighted graphs. *SIAM Journal on Imaging Sciences*, *10*(4), 1724-1766.

Odhengo, P., Lutta, A. I., Osano, P., & Opiyo, R., 2024: Urban green spaces in rapidly urbanizing cities: A socio-economic valuation of Nairobi City, Kenya. *Cities*, 155, 105430.

Ojobo, H., Oluwagbemiga, P. A., & Shamang, K. J., 2024: Unveiling the Impact of Urban Green Landscape on Quality of Life in Kaduna, Nigeria: Residents' Perceptions and Sustainable Strategies. *Journal of Contemporary Urban Affairs*, 8(1), 16-36.

Oliveira, M., Santagata, R., Kaiser, S., Liu, Y., Vassillo, C., Ghisellini, P., ... & Ulgiati, S. (2022). Socioeconomic and environmental benefits of expanding urban green areas: A joint application of i-Tree and LCA approaches. *Land*, 11(12), 2106.

Pamukcu-Albers, P., Ugolini, F., La Rosa, D., Grădinaru, S. R., Azevedo, J. C., & Wu, J. (2021). Building green infrastructure to enhance urban resilience to climate change and pandemics. *Landscape Ecology*, 36(3), 665-673.

Rodríguez González, K. D., Yépez-Rincón, F. D., Treviño Carreón, J., Zapata Wah, I., Ferriño Fierro, A. L., Aguilar Treviño, C., Vega Aguilar, A., Huerta García, R., and Antonio Durán, Y. Z. (2025). An UAV for 3D Tree Surveying Method as an Improvement for Dam Construction Environmental Impact Manifestation in Mexico, *ISPRS Annals of the Photogrammetry*

Remote Sensing Spatial Information Sciences, X-2/W2-2025, 157–164, https://doi.org/10.5194/isprs-annals-X-2-W2-2025-157-2025, 2025.

Vargas-Hernández, J. G., & Zdunek-Wielgołaska, J. (2021). Urban green infrastructure as a tool for controlling the resilience of urban sprawl. *Environment, Development and Sustainability*, 23(2), 1335-1354.

Vega Aguilar, A., Yépez-Rincón, F. D., Rodríguez Gonzalez, K. D., Vázquez Rodríguez, D. A., Ferriño Fierro, A. L., and Guerra Cobián, V. H. (2025). UAV for flooding risk assessment in a new Dam Construction in Northeast Mexico, *ISPRS Annals of the Photogrammetry Remote Sensing Spatial Information Sciences*, X-2/W2-2025, 189–197, https://doi.org/10.5194/isprs-annals-X-2-W2-2025-189-2025, 2025.

Verdú-Vázquez, A., Fernández-Pablos, E., Lozano-Diez, R. V., & López-Zaldívar, Ó. (2021). Green space networks as natural infrastructures in PERI-URBAN areas. *Urban Ecosystems*, 24, 187-204.

Wang, J., Wang, W., Zhang, S., Wang, Y., Sun, Z., & Wu, B. (2023). Spatial and temporal changes and development predictions of urban green spaces in Jinan City, Shandong, China. *Ecological Indicators*, 152, 110373.

Xi, Z., & Hopkinson, C. (2022). 3D graph-based individual-tree isolation (Treeiso) from terrestrial laser scanning point clouds. *Remote Sensing*, 14(23), 6116.

Yan, F., Xia, E., Li, Z., & Zhou, Z. (2021). Sampling-based path planning for high-quality aerial 3D reconstruction of urban scenes. *Remote Sensing*, 13(5), 989.

Yang, B., Ali, F., Zhou, B., Li, S., Yu, Y., Yang, T., & Zhang, K. (2022). A novel approach of efficient 3D reconstruction for real scene using unmanned aerial vehicle oblique photogrammetry with five cameras. *Computers and Electrical Engineering*, 99, 107804.

Zhang, F., & Qian, H. (2024). A comprehensive review of the environmental benefits of urban green spaces. *Environmental Research*, 118837.

Zheng, J.; Fu, H.; Li, W.; Wu, W.; Yu, L.; Yuan, S.; Tao, W.Y.W.; Pang, T.K.; Kanniah, K.D. (2021) Growing status observation for oil palm trees using Unmanned Aerial Vehicle (UAV) images. *ISPRS Journal of the Photogrammetry Remote Sensing*, 173, 95–121.

Ziter, C. D., Pedersen, E. J., Kucharik, C. J., & Turner, M. G. (2019). Scale-dependent interactions between tree canopy cover and impervious surfaces reduce daytime urban heat during summer. *Proceedings of the National Academy of Sciences*, 116(15), 7575-7580.

Zhang, W., Qi, J., Wan, P., Wang, H., Xie, D., Wang, X., & Yan, G. (2016). An easy-to-use airborne LiDAR data filtering method based on cloth simulation. *Remote Sensing*, 8(6), 501.